International Journal of Biological Macromolecules 319 (2025) 145457

Contents lists available at ScienceDirect

International Journal of Biological Macromolecules

journal homepage: www.elsevier.com/locate/ijbiomac

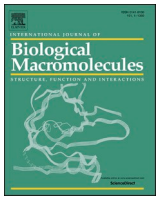

Environmentally friendly upcycling of PHA-based copolymers

Giacomo Damonte [a], Martina Cozzani [a], Marco Ozenda [a], Chiara Siracusa [b,c], Maria Jose Calandri [a], Alessandro Pellis [a], Georg M. Guebitz [b,c], Orietta Monticelli [a,*]

[a] Universitá degli Studi di Genova, Dipartimento di Chimica e Chimica Industriale, Via Dodecaneso 31, 16146 Genova, Italy
[b] Institute of Environmental Biotechnology, Department of Agricultural Sciences, BOKU University, Konrad-Lorenz-Strasse 20, 3430 Tulln an der Donau, Austria
[c] Austrian Centre of Industrial Biotechnology, Konrad-Lorenz-Strasse 20, 3430 Tulln an der Donau, Austria

ARTICLE INFO

Keywords:
PHA
Recycling
Porous film

ABSTRACT

This work focuses on two fundamental aspects that make the use of plastics and, more recently, bioplastics sustainable and cyclical, namely their recycling and the valorization of the products resulting from this process. Poly(3-hydroxybutyrate-*co*-3-hydroxyhexanoate) (PHBH) was considered as substrate. A solventless partial chemical decomposition with concomitant branching was developed based on the use of reagents from renewable sources, namely pentaerythritol as polyalcohol and zinc stearate as catalyst. ^{1}H NMR, IR, and DSC measurements showed the formation of oligomers having a branched structure whose molecular weights and glass transition temperatures decreased with the increasing of the polyalcohol content in the reaction mixture. The oligomers were used as additives in the development of porous films based on the starting high molecular weight PHBH, exploiting a Non-Solvent Induced Phase Separation (NIPS) method using Cyrene®, a green solvent derived from cellulose. The ability of the films to retain a dye and the metal precursor palladium chloride was studied. In the latter case, the catalytic activity of the system consisting of Pd clusters formed on the porous substrate after the metal precursor reduction was demonstrated. Finally, the enzymatic hydrolysis of the films was evaluated using Humicola insolens Cutinase (HiC) at different concentrations and in different media.

1. Introduction

Polyhydroxyalkanoates (PHAs), a class of polyesters produced by bacteria as an intracellular carbon storage and energy source, are considered a viable alternative to oil-based plastics and have seen an exponential increase in their application in recent years [1] due to their biodegradability [2,3], biocompatibility [4], and low carbon footprint [5]. Among PHAs, poly(3-hydroxybutyrate) (PHB) is one of the most promising materials as it can be synthesized by microorganisms without further modification. However, due to the brittleness and low toughness of this homopolymer, copolymers of PHB additionally containing other hydroxy acids were developed to achieve better processability, higher ductility and better impact strength. In particular, copolymers such as poly(3-hydroxybutyrate-*co*-3-hydroxyvalerate) (PHBV) and poly(3-hydroxybutyrate-co-3-hydroxyhexanoate) (PHBH) could be a potential alternative to PHB, due to their improved ductility and thermal stability, displaying lower melting temperatures and wider processability windows [6–9]. In order to expand the application of PHBH and make its use sustainable and scalable, recycling strategies need to be considered, the development of which is still in its infancy and only a few cases have been reported. In general, it can be stated that the mechanical recycling of PHBH still poses several issues related to the reduction of the materials properties (i.e. molecular weight) and consequently of their performance.

Plozeau et al. [10] investigated for the first time the mechanical recycling of PHBH by five cycles of twin-screw extrusion. Despite the stability in terms of degradation temperature and chemical structure of the processed PHBH, size exclusion chromatography and melt flow index revealed a 24.3 % reduction in the molecular weight of the recycled materials, which were also characterized by a higher crystallinity compared to the starting polymer. In this light, the chemical recycling of PHBH can be seen as an interesting alternative to mechanical recycling, potentially generating a variety of small functional molecules. For example, Adachi et al. [11] investigated the pyrolysis of PHBH and some commonly used plastics, both alone and in mixtures. In particular, it was demonstrated that this biopolymer can be selectively pyrolyzed in a first separate step due to the lower degradation temperature (273–298 °C) compared to oil-based plastics (HDPE, PP, PS),

* Corresponding author.
E-mail address: orietta.monticelli@unige.it (O. Monticelli).

https://doi.org/10.1016/j.ijbiomac.2025.145457
Received 3 April 2025; Received in revised form 5 June 2025; Accepted 20 June 2025
Available online 23 June 2025

allowing the recovery of species derived from the degradation of its structure, such as propylene, isocrotonic acid, crotonic acid, 2-hexenoic acid, and their dimers. In a similar work, Shao et al. [12] studied the pyrolysis of PHBH at different temperatures (from 400 to 800 °C), with different concentrations of water vapor, evaluating the yield of pyrolyzate in the form of liquid and gaseous fractions. Indeed, it was found that the total recovery rate of the PHBH pyrolyzates ranged from 90.1 to 99.0 wt%, with the gaseous fraction increasing with the increase of the pyrolysis temperature. Despite the encouraging results of pyrolysis, it is worth underlining that this method requires a high energy input and leads to mixtures of compounds with low molecular weight and poorly controlled structures. Recycling approaches that consume less energy, limit the formation of mixtures, and ensure a more precise control of the products are thus of great application interest.

With this in mind, an alcoholysis process for PHBH was developed considering environmentally friendly aspects, such as the use of bio-based reagents that allow the formation of branched compounds with a high number of functional end groups, using a green chemistry-aligned approach. Compared to other recycling processes, our approach allows the final properties of the waste polymer to be modified while largely preserving the structure of its macromolecular chains, thus saving energy and reducing the number of steps required to obtain the desired functional materials. In addition, this approach will contribute to the development of new strategies for the circular economy by converting polymer waste directly into functional additives for new polymer materials. In particular, solventless reaction conditions and a procedure that does not require extensive work-up were attempted by using pentaerythritol (PE) as the polyol and zinc stearate ($Zn(St)_2$) as the catalyst. The reaction, which has been widely applied in the chemical recyclying process of other bioplastics, such as polylactic acid (PLA) [13] and polycaprolactone (PCL) [14], involves the transesterification reaction between the hydroxyl groups of PE and the ester bonds of PHBH and thus the green formation of branched oligomers with hydroxyl end groups was achieved. It is worth mentioning that the use of the above catalyst, which is frequently applied in cosmetics, in the polymer field as a lubricant [15] and as a transfer catalyst for the saponification of fats [16], is a novelty in the alcoholysis reaction of PHA-based materials. To close the material loop, the application of the oligomers obtained from alcoholysis was also investigated, taking into account their specific properties, i.e., their chemical nature and their peculiar geometry. These compounds were used as additives in the formulations of PHBH-based films, taking advantage of their compatibility with the polymer matrix and the potential ability to make the porous material, characterized by a highly functional surface area.

It is relevant to underline that PHBH-based porous films have never been studied, although they may offer several potential applications, as has been highlighted with other bioplastics such as polylactic acid (PLA) [17] or polycaprolactone (PCL) [18]. In particular, due to the fully biodegradable and biocompatible nature of this polymer, PHBH-based porous films may have high application potential in various fields, such as in the biomedical and environmental sectors, for example in the development of porous scaffolds for drug delivery or in the bioremediation of pollutants. To develop an easily scalable and environmentally friendly approach for the production of porous films, a simple Non-Solvent Induced Phase Separation (NIPS) method was applied using water as coagulant and Cyrene® (Cy) as solvent, a compound produced from renewable sources that has recently been effectively applied in the preparation of porous films based on PLA, polyethersulfone (PES), polyvinylidene fluoride (PVDF) and many other polymers [19–21]. In particular, the influence of the presence of oligomers prepared from different amounts of polyalcohol on the film properties in terms of morphology, thermal and mechanical properties, porosity and water uptake was investigated. In addition, the retention capacity of the films, which can be modified by the presence of the multifunctional additives, was investigated using an organic compound, namely pararosaniline hydrochloride (PR), a cationic triarylmethane dye [22] which mimics the behavior of amino-containing drugs and organic pollutants, and palladium chloride ($PdCl_2$) as source of an inorganic cation. The aim of the latter study was to prove the possibility of using the developed films as adsorbers for homogeneous catalysts thus demonstrating a potential and impactful application of our material. In order to further extend the application possibilities of the developed systems, the catalytic activity of the Pd/PHBH-based films was also evaluated after the reduction of the adsorbed metal precursor. The novelty of the work thus relates to different aspects: i) the proposed new recycling process, ii) the valorization of the materials from PHBH recycling by developing of novel porous films based on PHBH enriched with the star-shaped oligomers from its recycling, and iii) the application of the developed films as absorbers and in the catalytic field. Finally, not only the valorization of the recycled products was investigated, but also their influence on the degradability of the materials containing them, i.e., the PHBH-based films to which star-shaped oligomers from the recycling process were added, by means of enzymatic depolymerization tests (Fig. 1). This closed-loop upcycling approach, based on the production and use of functional oligomers to tailor the final properties of the polymer from which they are derived, could lay the groundwork for the development of a new class of sustainable materials with highly tunable properties, produced not only from PHA, but also from other virgin or waste polyesters.

2. Experimental section

2.1. Materials

Poly(3-hydroxybutyrate-*co*-3-hydroxyhexanoate) (PHBH) IamNature B6 A15 C (melt mass flow rate (MFR) at 165 °C, 5 kg load = 6 g/10 min) was purchased by Gruppo MAIP (Italy). Cyrene® (Cy) (≥98.5 %), Pentaerythritol (PE) (99 %), Palladium (II) chloride (≥99.9 %), Acetic acid (≥99.7 %), Sodium borohydride (≥98.0 %), Pararosaniline hydrochloride (PR), KPO buffer salts (KH_2PO_4 and K_2HPO_4), and (*R*)-3-hydroxybutyric acid (≥98.0 %) were purchased from Sigma-Aldrich and used as received. Technical grade ($Zn(St)_2$) was purchased from Faci S.p.A (Italy). *Humicola insolens* Cutinase (HiC) (Novozym 51032, product code: 06-3135) was purchased from STREM Chemicals.

2.2. Preparation of PHBH oligomers by alcoholysis

Branched PHBH oligomers were prepared from linear high molecular weight PHBH by an alcoholysis reaction. For this purpose, 10 g of PHBH pellets, previously dried in a vacuum oven at 30 °C for 3 days, were placed into a glass test tube reactor equipped with a stainless-steel stirrer, purged with Ar flow, and brought to 195 °C for 10 min to soft and mix the polymer. After this phase, PE was added in varying amounts (2, 5, or 10 wt%, based on the weight of the mixture composed of polymer, polyalcohol, and catalyst), depending on the desired molecular weight of the final branched additives. The system was then stirred at 160 rpm for 90 min to facilitate the PE dissolution in the polymer. After complete incorporation of PE, $Zn(St)_2$ (2 wt% based on the total weight of the mixture) was added as a catalyst to promote the transesterification reaction between PE hydroxyl groups and the ester bonds of PHBH. After the catalyst addition, the reaction was maintained for 60 min keeping the system under continuous stirring. Then, the molten additives were collected in a glass vial and stored in a desiccator before use. The samples prepared by alcoholysis were named according to the different PE amounts used for their preparation, e.g. sPHBH_PE2 denotes a branched polymer obtained by alcoholysis of PHBH using 2 % PE.

2.3. PHBH-based porous film preparation

To develop PHBH films, different PHBH solutions were prepared by dissolving PHBH polymer pellets in 10 mL of Cyrene® at 100 °C under stirring to reach a final concentration of 20 % *w/v* (e.g. 2 g PHBH in 10

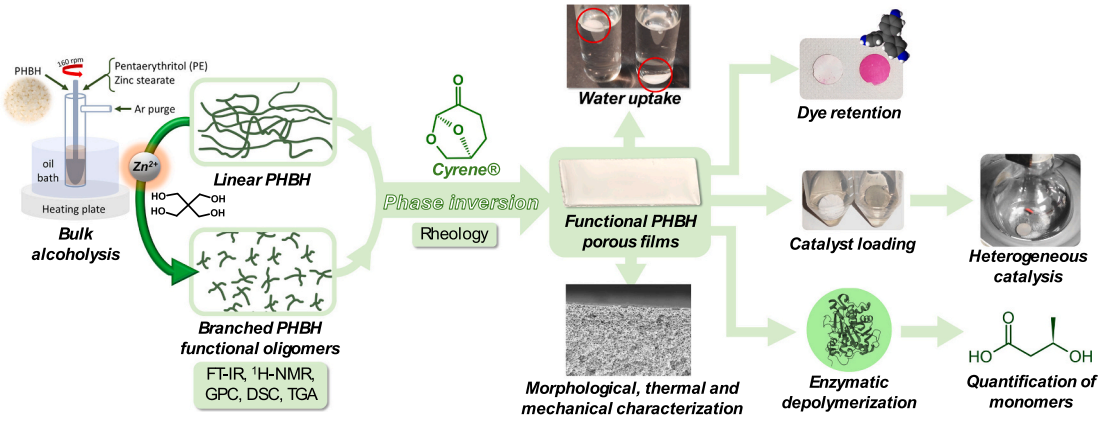

Fig. 1. Scheme of the work related to the development of a new recycling loop for PHBH-based materials.

mL solvent). To prepare functionalized films, PHBH and branched PHBH additives obtained by alcoholysis were mixed in a ratio of 80/20 % *w*/w to obtain solutions with a final polymer concentration of 20 % *w*/*v* (e.g. 1.6 g PHBH and 0.4 g additive in 10 mL solvent). Porous films were prepared by casting 10 mL of the hot PHBH/Cyrene® solutions, previously left at room temperature for 60 s, onto a glass plate using a doctor blade (film thickness = 1.1 mm, film width = 40 mm) and then by placing them in a coagulation bath of 450 mL Milli-Q water at 25 °C for 24 h after 30 s of additional air cooling. After this time, the films were detached from the glass plate and washed in water for 3 days, changing water several times a day and using the same amount of water as for the coagulation process. The as-prepared films were dried at room temperature for 72 h for three days and then in a vacuum oven at 30 °C for one week. The films were defined by specifying the type of the branched additive used in their preparation (e.g. mPHBH_PE2 indicates a film prepared from sPHBH_PE2 with a polymer concentration of 20 % *w*/*v* in Cy and a PHBH/sPHBH_PE2 ratio of 80/20).

2.4. Characterization measurements

2.4.1. FT-IR analysis

Fourier transform infrared spectroscopy was performed using a Bruker "Vertex 70®" in ATR mode, equipped with a diamond crystal, on powdered samples, at room temperature, from 400 to 4000 cm^{-1} (128 scan, resolution: 2 cm^{-1}).

2.4.2. NMR analysis

Proton NMR (^{1}H NMR) analysis of samples was carried out by using Bruker Avance 500 MHz spectrometer (Bruker, Karlsruhe, Germany) at 25 °C on 30 mg/mL polymer solutions prepared by dissolving the material in $CDCl_3$. The mean numerical molecular weight of polymers was calculated by applying Eq. (1) while the amount of PE esterified hydroxyl group was calculated using Eq. (2).

$$M_{nNM}[g/mol] = \left(\frac{A_{(b,e)}}{A_{(b',e')}} + 1\right) \cdot 89.16\ [g/mol] \quad (1)$$

where $A_{(b,e)}$ is the area of the signal at 5.25 ppm while $A_{(b'e')}$ is the area of the signal at 4.15 ppm. 89.16 g/mol is the mean molecular weight of the repetition unit which was extrapolated from the mean comonomer composition of 89 % 3-oxobutyric units (m.w. = 86.08 g/mol) and 11 % 3-oxohexanoic units (m.w. = 114.14 g/mol).

$$\text{Reacted OH groups respect total weight [\%]} = \frac{A_{i'}}{(A_i + A_{i'})} \cdot \text{pentaerythritol weight fraction [\%]} \quad (2)$$

where $A_{i'}$ is the area of the signal 4.06 ppm A_i is the area of the signal at 3.60 ppm.

2.4.3. Thermal analysis

DSC of the polymers and the prepared films was performed with a Mettler Toledo DSC1 STAR^e System. The analysis was carried out using a three-step thermal program composed respectively by a first heating (−50 °C to 200 °C), a cooling (200 °C to −50 °C) and a second heating (−50 °C to 200 °C). For all the steps, a heating/cooling rate of ±10 °C/min and a N_2 flow rate of 20 mL/min was used. TGA measurements were performed from 30 to 800 °C under a nitrogen flow of 80 mL/min using a heating rate of +20 °C/min.

2.4.4. GPC analysis

Gel permeation chromatography was carried out at 30 °C on an Agilent Technologies HPLC System (Agilent Technologies 1260 Infinity) connected to a 17,369 6.0 mm ID × 40 mm L HHR-H, 5 μm Guard column and an 18,055 7.8 mm ID × 300 mm L GMHHR-N, 5 μm TSK gel liquid chromatography column (Tosoh Bioscience, Tessenderlo, Belgium) using $CHCl_3$ as mobile phase (flow rate 1 mL/min). An Agilent Technologies G1362A refractive index detector was employed for detection. The molecular weights of the polymers were calculated using linear polystyrene calibration standards (250–70,000 Da) purchased from Sigma-Aldrich. Polymer samples were dissolved in $CHCl_3$, diluted to obtain a final concentration of 2 mg/mL, and filtered over cotton wool before analysis.

2.4.5. Viscosity analysis

The viscosities of the PHBH-based solutions used for film preparation were determined using a Lamy RM200 CP4000 plus® cone-plate rheometer with 40 mm spindle (CP40-20) at 100 °C, between 10 and 100 s^{-1}, whereby the average of 5 viscosity values was measured.

2.4.6. Gravimetric porosity

The porosity of the prepared films was determined using a gravimetrical technique, by applying Eq. (3).

$$\text{Porosity [\%]} = \frac{V_m - V_p}{V_m} \times 100 \quad (3)$$

where V_m is the sample volume calculated from the area and thickness of the film sample and V_p is the polymer volume within the film calculated by dividing the film sample weight by the polymer density (assuming that the density of PHBH and additives is identical, with $\rho_{PHBH} = 1.22$ g/cm^3).

2.4.7. SEM characterization

The morphological characterization of the porous films was performed using a Hitachi 3030 Scanning Electron Microscope (SEM). To

perform cross-section analysis, the film samples were fractured cryogenically after immersion in liquid nitrogen. All micrographs were acquired after applying a 3 nm thick platinum coating using a Leica ACE600 sputter coater. The pore size analysis of the materials was performed using ImageJ® software. The pore diameter was calculated based on an average of 50 measurements for each sample. The Pd-loaded films were coated with a thin graphite layer using a Polaron E5100 sputter coater and analyzed using a Zeiss Supra 40 VP field emission scanning electron microscope equipped with a backscattered electron detector. Pd cluster size was determined using the Feret's diameter function (the output is given as maximum Feret's diameter) of ImageJ® software.

2.5. Dye retention test

For the dye retention test, single film disks (diameter = 16 mm) were immersed in 5 mL PR solution (5 μg/mL), a dye that mimics the behavior of drugs and pollutants, in the dark at 22 °C for 48 h. After this time, the dye concentration in the leftover supernatant was quantified by UV–Vis spectrometry by measuring the absorbance at λ = 539 nm [23]. For PR quantification a calibration curve (Eq. (4)) was made using PR standards of different concentrations (0.5, 1, 2, 5, 10 μg/mL). The amount of dye retained at the time t was calculated using Eq. (5).

$$\text{Absorbance [a.u.]} = 0.21758 \cdot \text{Concentration } [\mu g/mL] + 0.02848 \; R^2 = 0.9977 \quad (4)$$

$$\text{Dye absorbed} = \frac{(C_0 - C_f) \cdot V_0}{w_{dry}} \quad (5)$$

where C_0 is the initial dye concentration [μg/mL], V_0 = 5 mL, C_f = measured dye concentration [μg/mL], w_{dry} = initial weight of the dried film disk (mg).

2.6. Water uptake measurements

The water uptake (WU) of porous PHBH films were measured by soaking single film disks (n = 3) in Milli-Q water at room temperature and weighing them at different time points. The amount of retained water at the time t was calculated using Eq. (6).

$$WU\,[\%] = \frac{w_t - w_0}{w_0} \bullet 100 \quad (6)$$

where w_t and w_0 are the weight of the soaked film after time t and the initial weight of the dry film, respectively.

2.7. Stress-strain test

Strain tests were performed with an Instron Mechanical Tester (Instron 5565) (speed 0.5 mm/min, initial gage length l_0 = 20 mm, pre-strain 0.1 N) on 30x5x0.45 mm^3 specimens cut perpendicular to the casting direction. All the samples were dried and stored in a desiccator over activated 4 Å molecular sieves at room temperature for 72 h before testing.

2.8. Palladium retention

Single film disks (diameter = 16 mm, mean thickness = 0.45 mm) were soaked for 48 h at room temperature in 3 mL of a 0.01 % *w/v* $PdCl_2$ solution in 0.5 % *v*/v acetic acid. After palladium absorption, the disks were washed three times with Milli-Q water, immersed in Milli-Q water for 10 min, and vacuum-dried until a constant weight was reached. After this phase, the loaded disks were immersed in 0.1 M aqueous $NaBH_4$ for 60 min to achieve the reduction and deposition of Pd^{2+} to Pd^0. Then, the samples were washed extensively to remove the excess of the reducing agent and dried under vacuum to constant weight. The Pd content of the films was determined by flame absorption atom spectroscopy (FAAS). In detail, single film disks (diameter = 16 mm, mean thickness = 0.45 mm) were dissolved in 1.5 mL of warm aqua regia (70 °C, closed vessel) prepared by mixing concentrated nitric acid (65 % *w*/w) and hydrochloric acid (37 % w/w) in a ratio of 1:3. After 24 h of digestion, the solutions were analyzed. The Pd concentration was determined using FAAS (Pd lamp, λ = 244.8 nm) preparing a calibration curve (Eq. (7)) using Pd standards at different concentrations (0, 1, 2, 5, 10, 20, and 50 μg/mL Pd using $PdCl_2$) in aqua regia. The amount of retained Pd was calculated by applying Eq. (8).

$$\text{Absorbance [a.u.]} = 0.032 \cdot \text{Concentration } [\mu g/mL] - 3.333 \cdot 10^{-4} \; R^2 = 0.9977 \quad (7)$$

$$\text{Pd absorbed} = \frac{C_{Pd} \cdot V_0}{w_{dry}} \quad (8)$$

where C_{Pd} is the Pd concentration measured by FAAS (μg/mL), V_0 = 5 mL, w_{dry} = weight of the dried film disk (mg).

2.9. Evaluation of the catalytic activity of Pd-loaded films

To evaluate the catalytic activity of Pd-loaded films and validate their use as catalytic supports, the materials were studied as heterogeneous catalysts to promote the hydrogenation reaction of trans-stilbene and compared to Pd/C. In detail, a single film disk (Ø = 16 mm) of Pd-loaded film (or 1.6 mg of Pd/C, Pd content = 10 wt%) was inserted into a 250-mL three-neck round-bottomed flask followed by a solution containing 375 mg of trans-stilbene dissolved in 8.3 mL of iPrOH, and the air present in the system was removed by carrying out three vacuum/nitrogen cycles. The hydrogen was then introduced into the reactor through a rubber balloon, performing three vacuum/hydrogen cycles and the reaction continued for 24 h. The conversion of trans-stilbene to diphenylethane was determined using ^1H NMR spectroscopy after solvent removal using a rotavapor and dissolution of the resulting solids in $CDCl_3$. The catalytic activity of Pd-loaded films and Pd/C was determined by using Eq. (9).

$$\text{Catalyst activity } [mg^{-1}] = \frac{\textit{Diphenylethane yield}}{\text{Pd weight [mg]}} \quad (9)$$

2.10. Enzymatic hydrolysis of films

Enzymatic hydrolysis of films was performed by placing single film specimens (5 × 10 mm^2, mean weight 5.8 ± 0.7 mg, n = 3) in a 2 mL Eppendorf tube, followed by 2 mL of HiC solution (Novozym®) 51.032 (1 or 5 μM) in Milli-Q water or 0.1 M KPO buffer, pH = 8.0. The films samples were then incubated for 1, 2, 5, and 10 days at 37 °C on an orbital shaker set to 150 rpm. At the specified time, the clear supernatant was collected after centrifugation at 5000 rpm for 5 min to remove suspended particles. The film residues were washed twice by immersion in 1 mL ultrapure water for 30 min each time and recovered by centrifugation. The residues were then vacuum-dried at room temperature for 3 days until constant weight was reached, before weight loss was determined gravimetrically on an analytical scale (±0.00001 g).

2.11. Quantification of hydrolysis products using RP-HPLC-RI

Hydrolysates (200 μL) were diluted to 980 μL using Milli-Q water and precipitated following the Carrez method [24] (10 μL potassium hexacyanoferrate solution +10 μL zinc sulfate solution) to remove the remaining enzyme and filtered through 0.20 μm Nylon filters (GVS, Indianapolis, USA). The analytes were separated by high-performance liquid chromatography (HPLC) using refractive index detection (1100 series, Agilent Technologies, Palo Alto, CA) coupled with an ICSep-ION-300 column (Transgenomic Organic, San Jose, CA) of 300 mm by 7.8

mm and 7 μm particle diameter. Column temperature was kept at 45 °C. Samples (40 μL) were injected and separated by isocratic elution for 110 min at 0.325 mL/min in 0.01 M H_2SO_4 as the mobile phase. A (*R*)-3-hydroxybutyric acid (3-HBA) calibration curve going from 1 to 20 mM (Eq. (10)) was used for the quantitative determination of the released 3-HBA during enzymatic hydrolysis of films.

$$\text{Absorbance [a.u.]} = 82,986 \cdot \text{Concentration } [\mu g/mL] \; R^2 = 0.9751 \qquad (10)$$

3. Results and discussion

3.1. Study of the alcoholysis reaction

Alcoholysis of commercially available linear poly(3-hydroxybutyrate-*co*-3-hydroxyhexanoate) (PHBH) to obtain branched oligomers was carried out in the molten state under solventless conditions. Pentaerythritol (PE), a biobased polyalcohol, was combined with Zn $(St)_2$ as a catalyst to promote the transesterification reaction between the hydroxyl groups of PE and the ester bonds of PHBH. To better evidence the influence of PE on the alcoholysis process, increasing amounts of this compound, namely 2, 5, and 10 wt% were used. In Fig. 2, the FT-IR spectrum of neat PHBH is compared with those of samples treated with different amounts of PE in the presence of $Zn(St)_2$ as a catalyst. The spectrum of PHBH exhibits characteristic stretching signals at 2981 cm^{-1} and 2939 cm^{-1}, which can be attributed to symmetric and asymmetric CH_2 stretching, respectively, and a prominent band at 1724 cm^{-1} corresponding to the C═O stretching. Additional peaks at 1457 cm^{-1} and 1382 cm^{-1} are related to CH_2 and CH_3 vibrational motions, while signals at 1277 cm^{-1} and 1181 cm^{-1} can be ascribed to asymmetric C—O—C and C—O stretching [10]. The peaks in the region between 1100 cm^{-1} and 500 cm^{-1} are attributed to C—O and C—C stretching in the amorphous phase [25].

All samples subjected to the alcoholysis process exhibited an additional absorption band between 3600 cm^{-1} and 3100 cm^{-1}, attributed to O—H stretching with the intensity of this band increasing with the PE content in the reaction mixture. Moreover, a detailed comparison of the spectra in the 4000 to 3000 cm^{-1} range (Fig. S1) reveals that the O—H stretching band in the polymer samples subjected to alcoholysis appeared broadened and shifted towards higher wavenumbers when compared to crystalline PE, suggesting a different nature of the hydroxyl end groups. Indeed, this indicates a possible disruption of the hydrogen bonds between hydroxyl end groups in the polymer matrix, which, as already reported, proves the occurrence of the transesterification reaction [13,26].

^{1}H NMR spectroscopy, reported in Fig. 3a and b, investigated the structural changes induced by the alcoholysis process in the resulting oligomers. In the spectrum of the starting linear PHBH, several signals can be recognized that can be assigned to the backbone protons of this polymer, namely at: 5.26 ppm (b, e), 2.61–2.49 ppm (a, d), 1.58 ppm (f, g), 1.28 ppm (c), and 0.91 ppm (h). Moreover, by comparing the areas of the signals c and h, which correspond to the methyl groups of the 3-oxobutyric and 3-oxohexanoic units, respectively, it was found that the copolymer composition consists of approximately 89 % 3-oxobutyric units and 11 % 3-oxohexanoic units. Additionally, as reported by Tripathi et al. [27], the lack of separation in the signals corresponding to protons b and e, which are attributed to the methine protons of 3-oxobutyric and 3-oxohexanoic units, respectively, suggests a random copolymer structure for this polyester. Similarly, all the samples prepared by alcoholysis showed the typical pattern of signals previously observed for the PHBH backbone, at 5.28 ppm (b, e), 2.65–2.56 ppm (a, d), 1.60 ppm (f, g), 1.28 ppm (c), and 0.91 ppm (h). Additionally, new signals attributable to PE and new chain end groups resulting from the alcoholysis reaction of PHBH at 4.20 ppm (methine protons of 3-hydroxybutyric and 3-hydroxyhexanoic chain terminals, depicted as b′ and e′, respectively) can be observed in these samples. Other peaks can be attributed to the presence of PE at 4.12 ppm (i′), 3.63 ppm (i), and 3.22 ppm (j). Moreover, other signals at 6.97 and 5.79 ppm, can be associated with the vinyl protons of 2-butenoic and 2-hexenoic units, respectively, with the peaks at 2.14 ppm and 1.88 ppm related to the methylene and methyl groups adjacent to the double bond of the 2-hexenoic (hex.) and 2-butenoic (but.) systems. These signals show an intensity that depends on the amount of added polyol and consequently on the progress of the alcoholysis process. The formation of these species can be explained by considering a partial dehydration reaction of the hydroxy end groups, which can be favored by the high temperature and the presence of the Lewis acid catalyst used for the transesterification. However, the

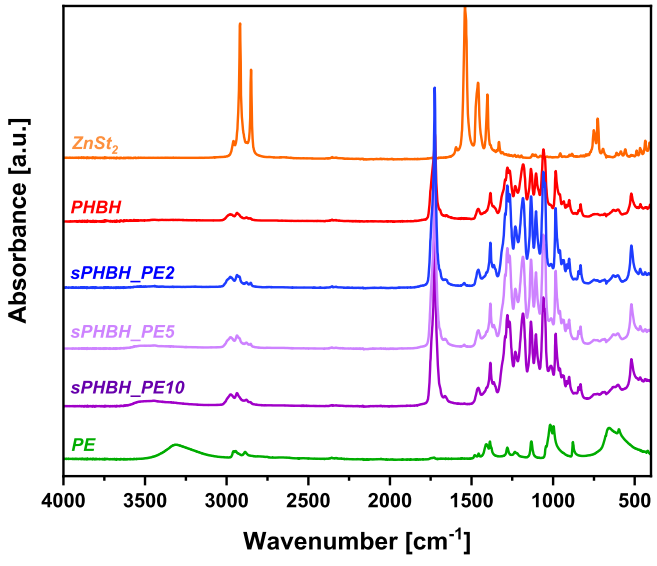

Fig. 2. FT-IR spectra of PHBH, PE, $Zn(St)_2$, and PHBH-based branched oligomers prepared by alcoholysis using PE and $Zn(St)_2$.

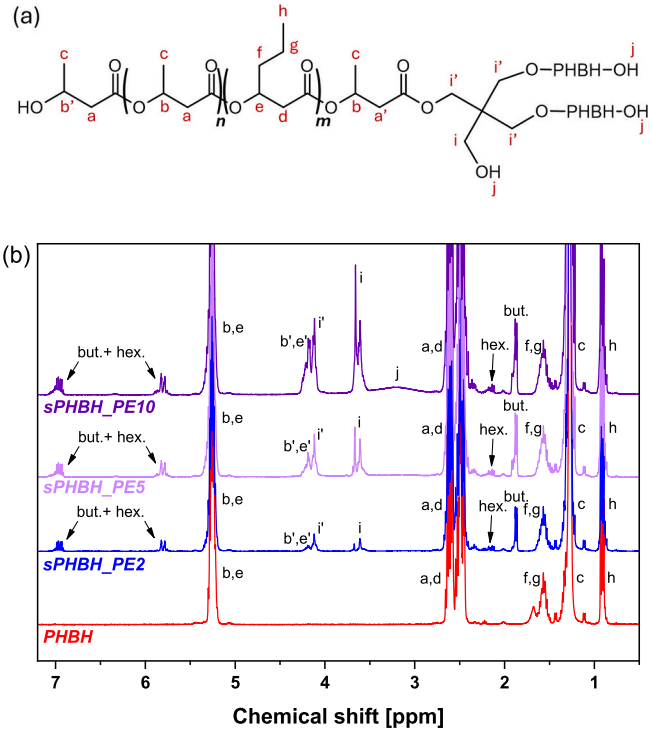

Fig. 3. Example of a possible structure of a trifunctional branched PHBH oligomer obtained from the alcoholysis reaction of linear PHBH using PE (a) and ^{1}H NMR spectra of PHBH and PHBH branched oligomers prepared by alcoholysis using PE and $Zn(St)_2$ (b).

presence of these functionalities, derived from α,β-unsaturated compounds, are present in minor amounts compared to the hydroxyl chain terminals, which are the primary focus of this study.

The molecular weight of the branched PHBH oligomers (Table S1) was calculated by applying Eq. (1). The linear starting PHBH was characterized by a high molecular weight and had an M_{nNMR} value of about 190,000 g/mol. After the alcoholysis reaction, a drastic decrease in molecular weight to 3700 g/mol, 1200 g/mol, and 500 g/mol was observed for the samples prepared by adding 2 %, 5 %, and 10 % PE, respectively, demonstrating the active role of the polyalcohol/catalyst system used in the transesterification.

Moreover, the area of (i) and (i′), i.e. the signals related to the methylene protons of free and esterified hydroxyl groups of PE, was dependent on the amount of PE added to the system, and was used to determine the number of hydroxyl groups involved in the reaction with PHBH chains during alcoholysis (Eq. (2)). When the proportion of esterified hydroxyl groups relative to the total weight of the system is considered, it is found that the values were 1.0 %, 3.0 %, and 3.4 % for sPHBH_PE2, sPHBH_PE5, and sPHBH_PE10, respectively. This indicates that a larger number of reacted hydroxyl groups are present in the systems with increasing PE content. This result highlights that in the case of sPHBH_PE10, a higher content of esterified groups indicates a greater extent of the alcoholysis process of PHBH, which is consistent with the observation made due to the decrease in molecular weight of the branched systems. Based on the above results, it can be concluded that alcoholysis successfully leads to the formation of branched structures with terminal hydroxyl groups and offers the possibility to adjust the final properties of the materials by varying the PE content used in the process.

GPC analysis (Fig. S2 and Table 1) was performed to assess the effect of the alcoholysis reaction on the molecular weight of the synthesized oligomers. Indeed, the alcoholysis was found to produce a significant reduction in the mean numerical molecular weight (M_n) of the polymer which decreased from 126,800 g/mol for the neat PHBH to 2300 g/mol, 1800 g/mol, and 1400 g/mol for sPHBH_PE2, sPHBH_PE5, sPHBH_PE10 respectively.

This result is consistent with the previously described findings from ^{1}H NMR analysis and demonstrates the effective conditions applied to obtain low molecular weights systems from linear PHBH [13].

Furthermore, a bell-shaped trend in polydispersity index (Đ) was observed as a function of the PE content used in the reaction, similar to what was reported by other authors who investigated the alcoholysis of PHB under different conditions and attributed the result to a possible random scission of the polymer chains during the process [28–30].

The thermal properties of the branched oligomers prepared by alcoholysis were compared with those of the starting PHBH using DSC measurements (Fig. S3, Table S2 and Table 1). In detail, DSC characterization of the neat polymer revealed a semicrystalline behavior, consistent with the composition of the copolymer, as reported elsewhere [31,32]. However, as evidenced by the small ΔH_c value of −3 J/g, PHBH can crystallize only to a limited extent under the cooling conditions used for the analysis. Moreover, this sample showed a T_g of −2 °C, a cold crystallization (ΔH_{cc}), and a fusion enthalpy of −33 J/g and 37 J/g, respectively, with low crystallinity (χ_c) of 3 %.

Table 1
Thermal properties of PHBH and branched PHBH oligomers.

Sample	T_g [°C]	T_{onset} [°C]	T_{max} [°C]	M_n [g/mol]	M_w [g/mol]	Đ
PHBH	−2	299	308	126,700	245,900	1.94
sPHBH_PE2	−9	288	301	2270	4690	2.06
sPHBH_PE5	−13	287	303	1790	3120	1.74
sPHBH_PE10	−16	287	305	1350	1960	1.44

T_g = glass transition temperature, *T_{onset} was extrapolated from TGA using the tangent method. T_{max} was extrapolated from DTG curves as the points where the mass loss rate was at its maximum.

In contrast, all samples prepared through the alcoholysis did not crystallize under the same cooling/heating conditions. In particular, in the second heating, no cold crystallization event was observed. Furthermore, a significant reduction in T_g was observed in all these samples compared to the initial PHBH, decrease which is related to the PE content added to the reaction mixture. These results can be attributed to several effects, such as the extent of the alcoholysis process, the branched geometry, and the possible plasticizing effect of the catalyst and free PE moieties. Indeed, the physical appearance of the samples also supports these findings; while the neat PHBH is in the form of hard, solid pellets at room temperature, all the branched oligomers are waxy materials that can be easily scraped off with a spatula (Fig. S4).

TGA analysis (Fig. S5 and Table 1) further confirmed the effect of the alcoholysis process on the thermal stability of the oligomers. In particular, PHBH exhibited an onset decomposition temperature (T_{onset}) of 299 °C and a maximum decomposition temperature (T_{max}) of 308 °C, reflecting the thermal stability determined for this polymer by other authors [33]. In contrast, the samples prepared by alcoholysis showed a slight reduction in thermal stability with T_{onset} of 288 °C, 287 °C, and 287 °C for sPHBH_PE2, sPHBH_PE5, and sPHBH_PE10, respectively. The maximum degradation temperatures (T_{max}) found for the oligomers, which were between 301 °C and 305 °C, showed a slight decrease compared to the 308 °C determined for the linear high molecular weight polymer.

The slight decrease in thermal stability observed in these samples was associated with the lower molecular weight compared to the neat polymer and the presence of the catalyst used to promote the transesterification process, which could favour earlier depolymerization and thus degradation of the material [34]. However, the thermal stability of the oligomers, although slightly lower, is still acceptable and comparable to that of the starting PHBH. Overall, these findings highlight the influence of the alcoholysis process on the final properties of the oligomers and demonstrate how effectively the transesterification reaction promotes the cleavage of the macromolecular chains to generate branched structures characterized by terminal hydroxyl groups.

3.2. PHBH-based porous film development

To highlight a potential application, the compounds derived from the PHBH alcoholysis process were used as additives in the development of PHBH-based porous films, taking advantage of their compatibility with the polymer matrix and their high functionality, as already underlined. In the film development, both the neat PHBH and the mixture of PHBH and branched oligomers obtained by using different amounts of PE were dissolved in Cyrene® (Cy), a solvent produced from renewable sources. The choice of this compound compared to other solvents used for the production of porous films, such as dimethyl sulfoxide (DMSO) and dimethylformamide (DMF), is not only related to its bio-based nature, but also to its peculiar chemical-physical characteristics (high viscosity, miscibility with water, capacity to dissolve the polymer) which make Cy suitable for its application in a Non-Solvent Induced Phase Separation (NIPS) process.

The study of the development of such materials initially focused on analyzing the viscosity of the polymer solutions used to produce the films, as this parameter is of fundamental importance for the formation of the porous material in the method applied [35]. It is worth underlining that Cy has never been used in the preparation of PHBH-based films, so it was not possible to compare the viscosities found with the values reported in the literature. As shown in Fig. S6, the η value of the solution characterized by a polymer concentration of 20 % *w/v* and measured at 100 °C, i.e., at the temperature applied to dissolve the polymer, decreased drastically after the addition of the branched oligomers, from about 1200 mPa·s, for the PHBH solution to about 500 mPa·s for those containing the additives. The reduction in viscosity caused by the presence of the oligomers in the systems can be attributed to their low molecular weight. In this context, it is relevant to underline

that the addition of the low-molecular weight branched oligomers causes a reduction in the high molecular weight PHBH content since the total concentration of the polymer was maintained at 20 wt% in all the solutions studied. However, no significant changes in η value were observed because the difference in molecular weight between the three branched oligomers, sPHBH_PE2, sPHBH_PE5, and sPHBH_PE10, is not so relevant. Based on the above results, it is worth underlining that despite the decrease due to the presence of the branched oligomers, the viscosity of the prepared polymer solutions remains acceptable and within a range suitable for application in a NIPS process [36,37].

To evidence the influence of the viscosity of the starting solutions on the porosity of the films, the density of the materials was measured. In Fig. S6, the gravimetric porosity of the neat PHBH and that of PHBH/branched oligomer films are shown. The porosity was found to be similar for all the studied systems, it being 73.4 ± 2.7, 78.8 ± 1.8, 79.6 ± 3.0, and 77.1 ± 1.2 for mPHBH, mPHBH_PE2, mPHBH_PE5, and mPHBH_PE10, respectively. This finding can be attributed to the fact that the differences in viscosity between the solution based on the neat PHBH and those with the PHBH/branched oligomer systems are not so great - almost half in the case of the latter - as to justify a significant change in porosity, as demonstrated in other works [38]. Nevertheless, it is relevant to underline that the use of the above solvent-polymer systems allows the production of films with medium-high porosity values, which are optimal for their use as pollutant absorbers or porous supports for catalysts [39].

FE-SEM characterization of the cross sections of neat and composite PHBH-based porous films (Fig. 4) was carried out to evidence the influence of the branched additives on the film morphologies. In particular, a sponge-like porous morphology is observed along with a few tens of micrometers thick dense layer on the side directly exposed to water during the desolvation process (Fig. S7), which is formed because of a rapid spinodal demixing of the solution, as highlighted by other authors [40]. The analysis of the specimen prepared with neat polymer, mPHBH, revealed a mean pore area of 0.73 ± 0.21 μm. This value increased slightly to 0.93 ± 0.31, 0.94 ± 0.32 and 1.05 ± 0.37 μm for mPHBH_PE2, mPHBH_PE5, and mPHBH_PE10 respectively, with no statistically significant difference found for the addition of the oligomers characterized by different molecular weight. As previously demonstrated, the above results highlight the minor influence of the presence of the branched oligomers on both the film morphology and porosity.

The thermal properties of the prepared films were analyzed by DSC measurements (Fig. S8 and Table S3). During the cooling phase, none of the samples was able to crystallize effectively, as demonstrated by the low crystallization enthalpy (ΔH_c) values, which ranged between −4 J/g for the mPHBH film and −1 J/g for the films containing the additive. Due to the small and broad crystallization peaks, the crystallization temperatures (T_c) of these samples were poorly defined and ranged between 43 and 55 °C, with the lowest value for mPHBH and the highest

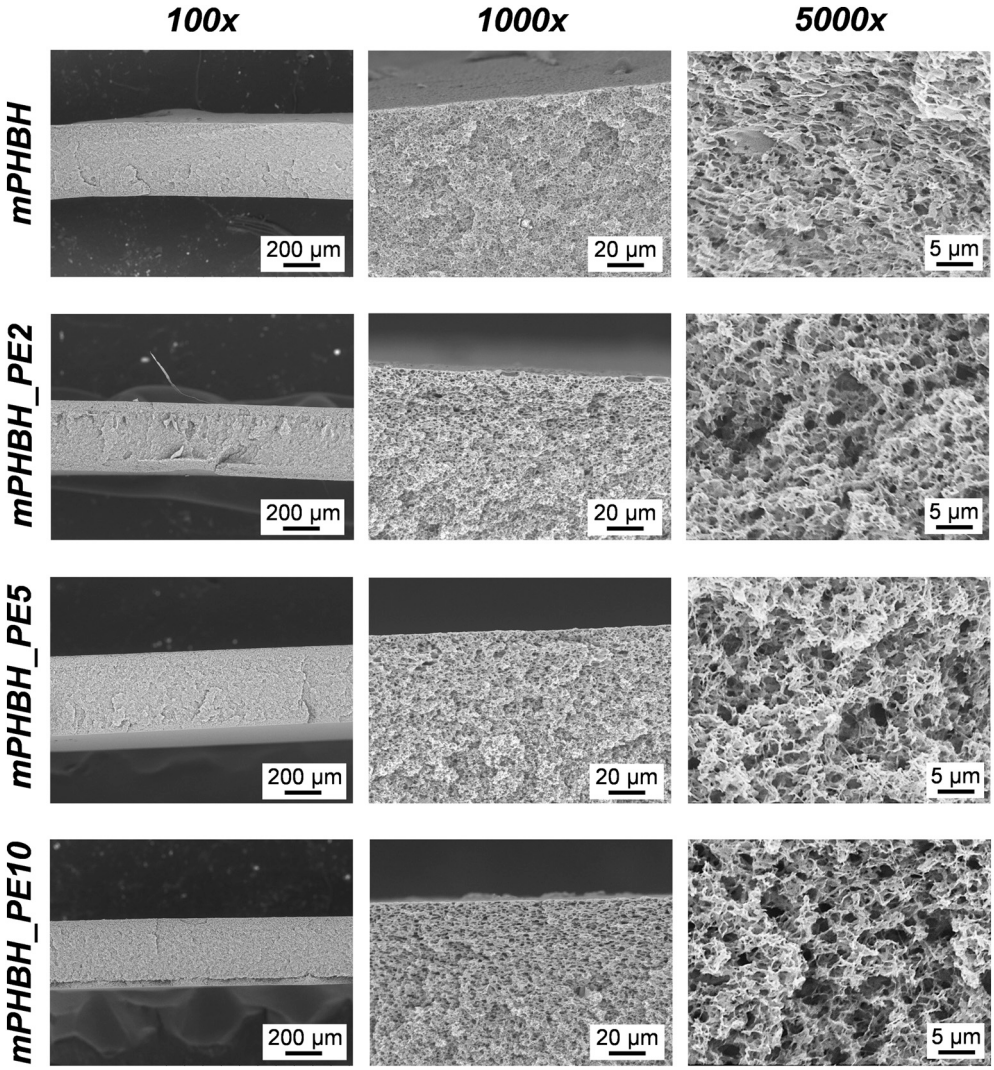

Fig. 4. SEM micrographs of PHBH-based film cross-sections at different magnifications.

for mPHBH_PE10. Concerning the thermograms of the second heating, glass transition temperature (T_g) values were found between −1 °C and −4 °C, for mPHBH and mPHBH_PE10 respectively, demonstrating how the addition of oligomers can decrease the temperature of this transition according to the Flory-Fox equation. Moreover, during the second heating phase, well above T_g, cold crystallization and melting processes were observed for all the films. As expected, the enthalpies associated with cold crystallization (ΔH_{cc}) and melting (ΔH_m) were comparable, further confirming the inability of these materials to crystallize efficiently under the applied cooling conditions. In addition, the temperature values for the cold crystallization and melting processes (T_{cc} and T_m) were almost the same for all the samples, demonstrating that the effect of the branched additives on these properties was relatively small.

The thermochemical stability of the films evaluated by TGA (Fig. S9 and Table S3) also evidenced that the values for the onset degradation temperature (T_{onset}) and the maximum rate of degradation temperature (T_{max}) were between 281–293 °C and 297–308 °C, respectively, indicating that the introduction of PHBH-based oligomers changes the thermal stability only slightly.

The mechanical properties of the neat PHBH films and those of the systems containing the branched oligomers were evaluated by stress-strain measurements; the results are shown in Table 2. In particular, Young's modulus, yield strength, and elongation at break of the sample mPHBH were found to be 43 ± 0.8 MPa, 1.09 ± 0.05 MPa, and 19.2 ± 2.9 % respectively, values well below those typically reported for dense PHBH specimens [3,41]. These results can be explained by considering the high porosity of the developed films, which limits the ability to transfer mechanical stresses across the material section. Characterization of the films containing branched additives yielded Young's modulus, tensile, and yield strength values comparable to those of high molecular weight mPHBH film. The most notable change observed in these materials was related to a reduction in elongation at break, which was approximately 6 % for all the films containing the oligomers. As reported by other authors, this effect can be attributed to a possible reduction in the entanglements between the polymer chains caused by the low molecular weight additives [42]. As demonstrated in the photographs, shown in the Supporting Information (Fig. S10), the manipulability of the above films remains excellent despite the significant reduction in this property, making these porous materials suitable for use as scaffolds or absorbers.

3.3. Study of the film retention capacity

The retention capacity of the functional PHBH films was evaluated using an organic compound, namely pararosaniline hydrochloride (PR) and palladium chloride ($PdCl_2$) as an inorganic cation. For the former compound, PR was selected based on previous studies showing that this molecule can be used to mimic the behavior of positively charged, amino-containing organic molecules, such as pharmaceuticals and pollutants [22,43]. To this end, the films were immersed in 5 μg/mL PR solution and the dye concentration in the supernatant was monitored after 24 and 48 h (Eq. (5) and Fig. 5). The dye adsorption of mPHBH and mPHBH_PE2 was relatively low after 24 h at 50 ± 36 μg/g and 46 ± 29 μg/g respectively. After 48 h, it increased to 87 ± 67 μg/g and 89 ± 27 μg/g, respectively. In contrast, mPHBH_PE5 and mPHBH_PE10 films showed significantly higher dye retention (Fig. S11), with values of 211 ± 67 μg/g and 331 ± 57 μg/g after 24 h, increasing to 330 ± 62 μg/g and 390 ± 70 μg/g after 48 h, respectively. The above findings highlight the low affinity of neat PHBH towards the dye, which is not even affected by the increase in the surface area of the support due to its porous structure in the film sample. To explain these results, the system functionalities, which can influence the affinity for the positively charged molecule as well as the water uptake (WU) must be taken into account. To better assess the latter aspect, gravimetric determination of WU over time was performed (Eq. (6) and Fig. 5). In particular, mPHBH showed a modest WU value, leveling off at 11 ± 3 % and 10 ± 1 % after 24 and 48 h, respectively. The mPHBH_PE2 sample also exhibited comparable WU after the same time (14 ± 2 % and 17 ± 5 %). Indeed, the low retention capacity of mPHBH and mPHBH_PE2 for PR can be attributed to the limited amount of functional end groups available for interactions with the selected molecule and for water uptake, which may facilitate the diffusion of PR within the porous structure. In contrast, the mPHBH_PE5 sample showed higher WU values of 58 ± 7 % and 106 ± 6 % over the time periods testes, which further increased to 226 ± 21 % and 218 ± 18 % in the mPHBH_PE10 sample, indicating a greater water absorption capacity (Fig. S12). The above variation cannot be related to the microstructure of the films, as the porosity as well as morphology, assessed by SEM micrographs, are the same for both samples.

Table 2
Stress-strain test of PHBH-based porous films.

Sample	Young's modulus [MPa]	Yield strength [MPa]	Elongation at break [%]
mPHBH	43.3 ± 0.8	1.09 ± 0.05	19.2 ± 2.9
mPHBH_PE2	42.6 ± 1.7	0.93 ± 0.07	6.0 ± 1.0
mPHBH_PE5	38.3 ± 0.3	0.76 ± 0.02	6.0 ± 0.4
mPHBH_PE10	48.1 ± 2.6	0.99 ± 0.01	6.3 ± 0.1

It is difficult to compare the WU values found with existing literature data, due to the novelty of PHBH-based porous films. However, it is worth underlining that the WU value of mPHBH_PE10 is in the same order of magnitude as that of other PHA-based porous polymer systems prepared by different strategies [44–46]. Considering the results of water uptake and the dye retention tests (Fig. 5), it is clear that they follow a similar trend, showing that the functionalities introduced by the presence of the branched oligomers in the PHBH-based films by the two compounds sPHBH_PE5 and sPHBH_PE10, characterized by the highest number of functional groups, promote dye retention through specific interactions and the dye adsorption within the porous structure thanks to the improved water uptake. Overall, these results show that although the additives are not able to improve the mechanical behavior of the film and even reduce the elongation at break without limiting the manipulability of the film, they have a strong influence on the retention capacity of the systems thanks to the functionality they confer. Even if a direct comparison with literature is difficult because there are no studies on films prepared with the same polymer/solvent pair, these results are consistent with some works in which a correlation was found between the content of polar groups introduced by the additives and the effectiveness of the film as an absorber of polar species [38].

As already highlighted, the retention capacity of the developed films was also investigated considering an inorganic salt which is used both in homogeneous catalysis [47], where it is dissolved in a suitable solvent system, and in heterogeneous catalysis as a metal precursor [48]. In particular, the aim of these measurements was to verify the possibility of using our materials as adsorbers of homogeneous catalysts, since one of the most challenging aspects of this type of catalysis is related to the separation of the catalysts from the reaction mixture dissolved in the same solvent system.

On this basis, the development of absorbers, possibly bio-based, that can limit the separation/purification steps is an aspect of great scientific and application interest. Likewise, we envisioned that our films could be reused as catalytic support after retention of the metal precursor and its reduction to develop a recycling strategy that could improve the applicability of our material.

For this purpose, two films were considered: a sample based on neat PHBH, mPHBH, and a film containing the branched oligomer, namely mPHBH_PE10 that showed the best performance in terms of PR retention compared to the other formulations analyzed. The analysis of the amount of Palladium retained revealed a clear difference between the two systems studied (Eq. (8)). Indeed, while the neat film was characterized by a negligible amount of retained Pd, mPHBH_PE10 showed a

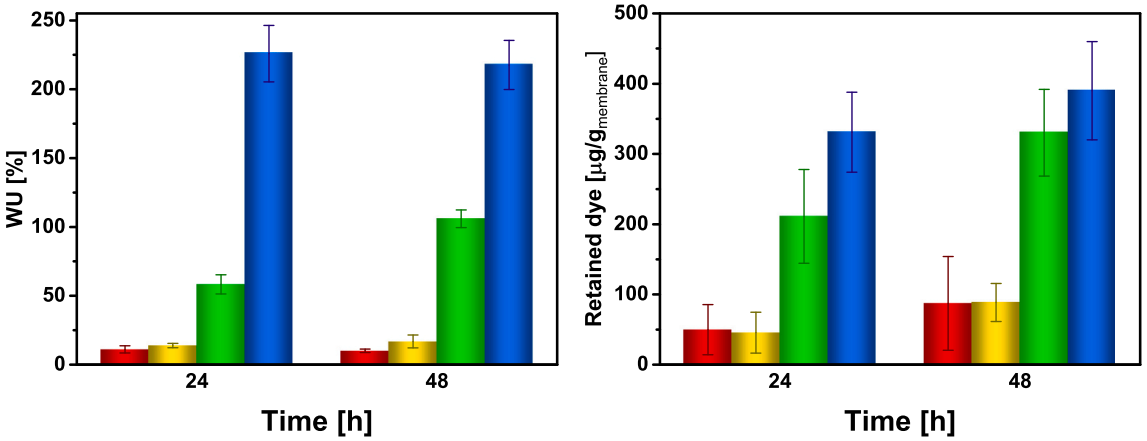

Fig. 5. WU and PR retention of PHBH-based porous films vs. time, at 22 °C of: mPHBH (red), mPHBH_PE2 (yellow), mPHBH_PE5 (green), and mPHBH_PE10 (blue).

significant retention with an adsorbed amount of 1.48 µg Pd/$mg_{dry\ film}$. Since only very small amounts of Pd are normally used in homogeneous catalysis (from 1 % to 4 % mol in relation to the reagents), this result shows the effectiveness of the developed materials as catalyst adsorbers.

In addition, it is worth underlining that the mPHBH_PE10 film (coded as mPHBH_PE10_Pd) appeared dark and had a homogeneous coloration after adsorption of the precursor, washing and reduction, while mPHBH was white and had the same initial coloration (Fig. S13). This difference cannot be attributed to the porosity of the films, as it was demonstrated that this property is not altered by the presence of the branched additive, but by the specific interactions that occur between the functional groups of the additive and the precursor. Furthermore, FE-SEM analysis of the dense and porous surfaces of the mPHBH_PE10_Pd sample (Fig. 6) shows the formation of metal clusters with dimensions of about 160 nm, measured as their maximum Feret's diameter. Again, a comparison with literature is difficult due to the novelty of the materials produced, but as with other polymer matrices, e.g. PLA or polyamides [49,50], the low ability to interact with catalytic precursors and the need to add organic or inorganic additives to the matrices, which can increase the affinity and retention of the polymer matrix towards these compounds, have been widely demonstrated.

To verify the reactivity of the mPHBH_PE10_Pd (Eq. (9)) system, its specific catalytic activity, calculated as conversion with respect to the amount of Pd, was compared with that of a commercial catalyst, Pd on carbon (Pd/C), in the hydrogenation reaction of a model compound, trans-stilbene (Fig. S14). Analysis of the reaction products after 24 h

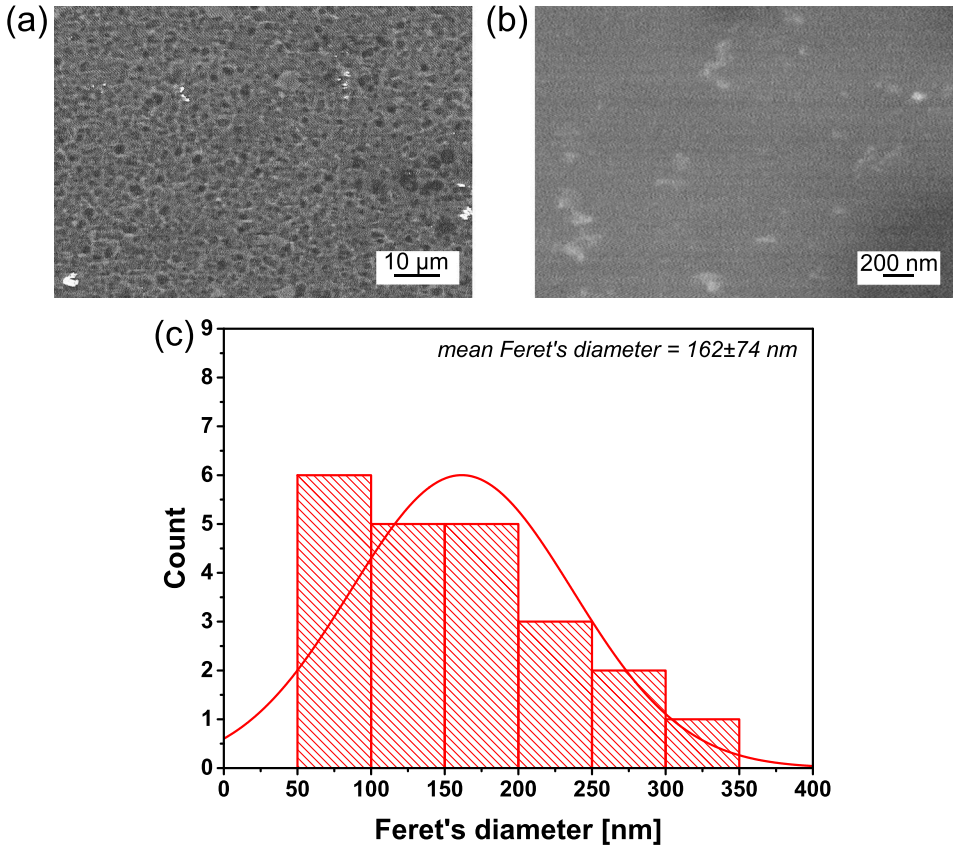

Fig. 6. SEM micrographs in backscattering mode of porous (a) and dense (b) side of mPHBH_PE10_Pd. Particle size analysis (max. Feret's diameter) of Pd clusters on mPHBH_PE10_Pd dense side (c).

showed a similar activity of 6.29 and 6.25 mg^{-1} for mPHBH_PE10 Pd and Pd/C, respectively.

This result is remarkable because it clearly demonstrates an effective and sustainable upcycling of PHBH to a functional catalytic material.

3.4. Enzymatic hydrolysis of films

The degradability of the developed films and the specific influence of the branched additives on this property were evaluated by monitoring the enzymatic hydrolysis with *Humicola insolens* cutinase (HiC). It is worth underlining that this enzyme, which has been shown to be highly active in the depolymerization of many types of polyesters, from those characterized by a purely aliphatic structure, such as PLA, PCL, and PBS to mixed aliphatic-aromatic ones such as PBAT and PEF and even polyamide [51,52], has never been assessed for the hydrolysis of PHBH.

In detail, the enzymatic hydrolysis of mPHBH and PHBH-based porous films (mPHBH_PE2, mPHBH_PE5, and mPHBH_PE10) at 37 °C, i.e., the physiological temperature, was investigated under different conditions to determine the influence of media type and enzyme concentration on their degradability. The experiments were carried out using Milli-Q water and KPO 0.1 M buffer at pH = 8.0 as the medium with HiC concentrations of 1 μM and 5 μM for 10 days. As shown in the histograms in Fig. 7, all materials exhibited minimal degradation in Milli-Q water with 1 μM HiC, reaching a mass loss of about 6 % for mPHBH, 6 % for mPHBH_PE2, 9 % for mPHBH_PE5, and 12 % for mPHBH_PE10 after 10 days of incubation. Increasing the enzyme concentration to 5 μM in the same medium led to a significant increase in mass loss for all films, with the percentage degradation after 10 days being approximately 24 % for mPHBH, 18 % for mPHBH_PE2, 30 % for mPHBH_PE5, and 34 % for mPHBH_PE10.

When the medium was changed to KPO buffer at pH 8.0 with 1 μM HiC, there was a moderate increase in degradation in all samples compared to 1 and 5 μM HiC in Milli-Q water. In detail, the mass loss measured after 10 days was approximately 20 % for mPHBH, 30 % for mPHBH_PE2, 28 % for mPHBH_PE5, and 32 % for mPHBH_PE10. However, the best depolymerization conditions were found to be in KPO buffer at pH = 8.0 with 5 μM HiC, where mass loss after 10 days was almost 74 % for mPHBH, 95 % for mPHBH_PE2, 99 % for mPHBH_PE5, with mPHBH_PE10 being completely depolymerized under these conditions. Moreover, these results also indicate that the mass loss is related to the composition and molecular structure of the materials. Indeed, mPHBH, i.e., the film composed entirely of high molecular weight linear polymer, was the most resistant to enzymatic hydrolysis. In contrast, the films prepared by adding 20 % wt% of a branched additive derived from the alcoholysis of linear PHBH (mPHBH_PE2, mPHBH_PE5, and mPHBH_PE10) showed higher hydrolysis than the pristine PHBH film. These results can be explained by the fact that, as already shown, increasing the amount of PE during alcoholysis reduces the molecular weight of the resulting additive and increases the number of hydroxyl groups. It can be hypothesized that the low molecular weight of the introduced oligomers, taking into account their insolubility in water, could shorten the total time required for the hydrolysis process, accelerating the mass loss of the oligomer-containing samples over time. As a direct consequence, mPHBH_PE10, i.e., the film with the highest PE content and the lowest molecular weight, consistently exhibited the highest susceptibility to enzymatic depolymerization of all the materials

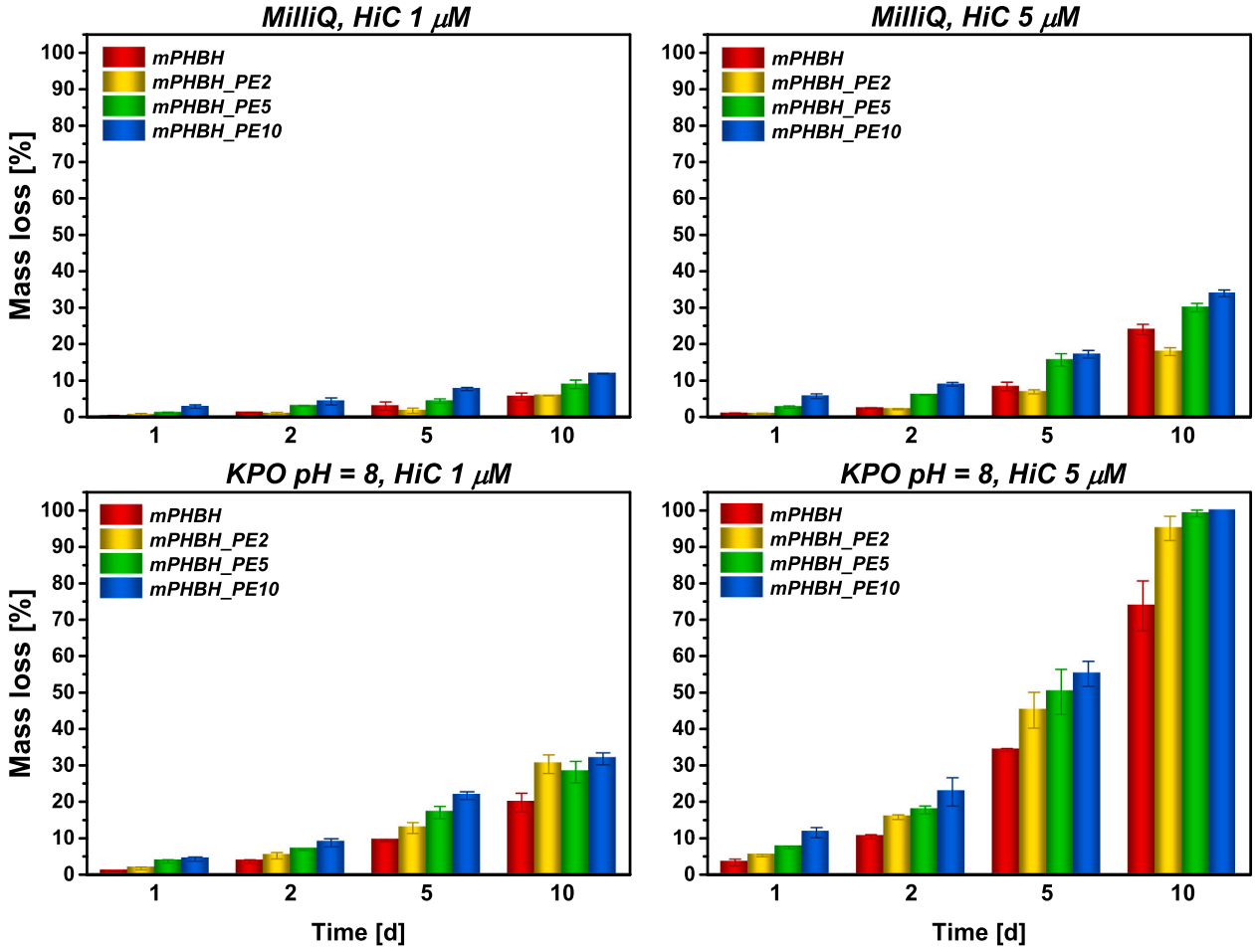

Fig. 7. Enzymatic hydrolysis of PHBH-based porous films using HiC in different concentrations and media, at 37 °C.

tested, followed by mPHBH_PE5 and mPHBH_PE2, with mPHBH being the slowest to degrade due to its linear, high molecular weight structure.

These findings were further supported by FT-IR analysis of mPHBH and mPHBH_PE10 samples (Fig. S15) after 5 days of degradation under different conditions. Indeed, in the 3100–3700 cm^{-1} range, mPHBH, showed an increase in absorbance compared to the starting film only when the material was subjected to hydrolysis with the HiC 5 μM KPO solution, i.e., under the strongest hydrolytic conditions. In contrast, in the case of the mPHBH_PE10 film, an increase in the absorbance was observed for both the samples treated with 1 and 5 μM HiC in KPO. As the above band can be associated with hydroxyl chain ends which can be formed during the enzymatic hydrolysis, the differences found are consistent with those previously observed from the mass loss data, highlighting the higher hydrolytic efficiency of enzymatic KPO buffer solutions and the greater susceptibility to hydrolysis of the additive-containing film. To better evidence the effect of enzymatic hydrolysis on film morphology, these samples were analyzed by SEM after 5 days of contact with the 5 μM HiC solution in KPO buffer at pH = 8.0 (Fig. 8). Under these conditions, mPHBH did not demonstrate significant changes in surface morphology on both the dense and porous sides, while mPHBH_PE10 exhibited some grooves along the surfaces, suggesting a possible collapse of the porous structure inside the film, which in turn indicates a higher degree of material erosion and hydrolysis.

RP-HPLC-MS analysis in positive ion mode of mPHBH and mPHBH_PE10 supernatants (Fig. S16 and Fig. S17), recovered after 10 days of hydrolysis with 5 μM HiC solution in KPO, revealed the presence of species resulting from the enzymatic depolymerization process of films. Molecular ions were found in both samples that can be assigned to monomeric (3-HBA monomer (M)) and oligomeric (3-HBA dimer (D) and trimer (T); mixed 3-HBA/3-HHA dimer (D_{mix}) and trimer (T_{mix})) species originated from PHBH chain hydrolysis. In addition, the formation of 3-HBA generated during this process was monitored by RP-HPLC-RI (Fig. 9, Fig. S18, and Fig. S19). As expected, the analysis of the supernatants obtained from the enzymatic hydrolysis of these materials again showed the presence of this compound, which was previously observed qualitatively by RP-HPLC-MS analysis. Since these materials consist mainly (~89 %) of 3-oxobutyric units, the presence of 3-HBA could be detected for all degradation times and under all the conditions used for the hydrolysis of the films. In particular, the evolution of 3-HBA in the supernatants showed a good correlation with the mass loss measured during the enzymatic hydrolysis tests, with the concentration increasing with time. Furthermore, when examining the individual time points of each sample, an increase in 3-HBA concentration was observed as a function of the capacity of enzymatic solutions in promoting the hydrolytic process, in the following order: 1 μM HiC Milli-Q < 1 μM HiC KPO < 5 μM HiC Milli-Q < 5 μM HiC KPO.

Remarkably, these results show that the enzymatic depolymerization process, for both 1 μM HiC solutions, does not occur under enzymatic saturation conditions, since the concentration of 3-HBA for each time point increases with the concentration of the enzyme in the transition to 5 μM solutions. In the same way, an increase in the concentration of 3-HBA was observed by switching from hydrolysis in Milli-Q water to buffer KPO. This phenomenon can be attributed to the influence of pH on the stability and ability of the enzyme to interact with the polymer surface, as well as to the buffering effect that the KPO can exert on 3-HBA, allowing the enzyme to work in an optimal pH range. These results are significant as they show for the first time that complete depolymerization of PHBH-based materials can be achieved in a reasonably short time (days) by using HiC and suggest that the degradation profile of films can be tuned by varying the type of branched oligomer used in their preparation or by modifying the conditions applied for hydrolysis in terms of enzyme concentration and medium. Moreover, these results can serve as potential indicators of the biodegradability of these materials and are also crucial for paving the way to explore future opportunities to develop a chemo-enzymatic recycling method for these materials at the end of their life cycle.

4. Conclusions

In this work, an efficient upcycling process for the valorization of PHA-based copolymers, namely PHBH, was developed under environmentally friendly conditions. The novel approach developed for the recycling of PHBH under solventless conditions was based on a transesterification reaction using bio-based compounds, namely pentaerythritol (PE) and zinc stearate, to promote the formation of oligomers with hydroxyl end groups and branched structure. The resulting branched PHBH oligomers exhibited a lower molecular weight and a lower T_g compared to the starting polymer, whereby the properties could be adjusted by changing the amount of PE in the reaction mixture. As for the valorization of the above compounds, they proved to be effective additives able to modify the properties and functionality of PHBH-based porous films - produced for the first time using a bio-based solvent, namely Cyrene® - thanks to their peculiar structure and compatibility with the polymer matrix. In particular, the oligomer-containing films, although characterized by a slightly reduced elongation at break compared to the neat PHBH-based films, proved to be

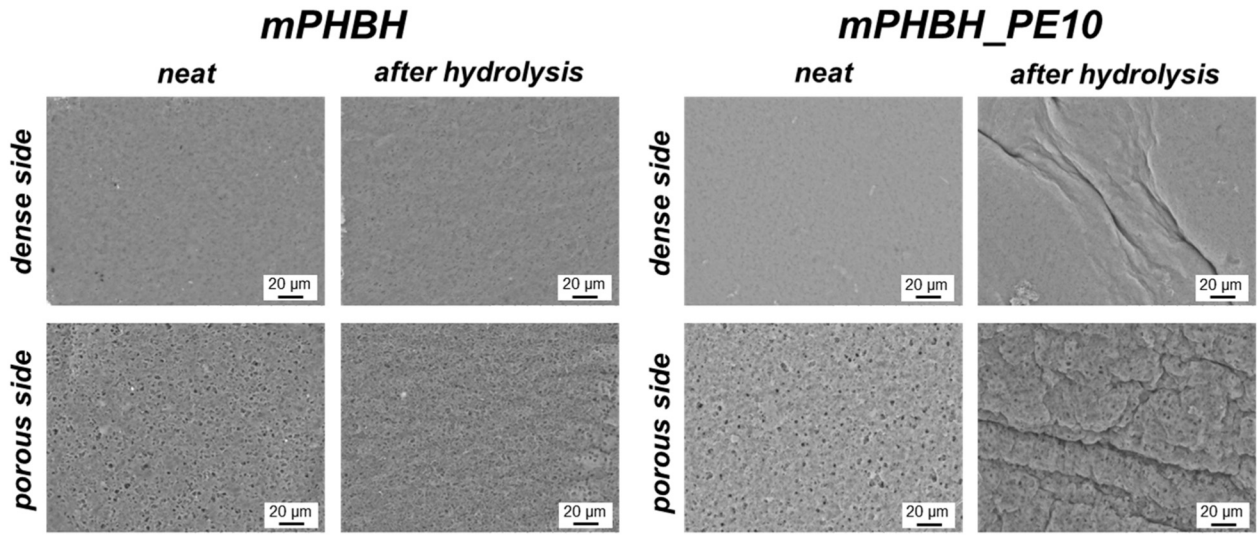

Fig. 8. SEM micrographs of dense and porous side of mPHBH and mPHBH_PE10 before and after 5 days of enzymatic hydrolysis using 5 μM in 0.1 M KPO buffer, pH = 8.

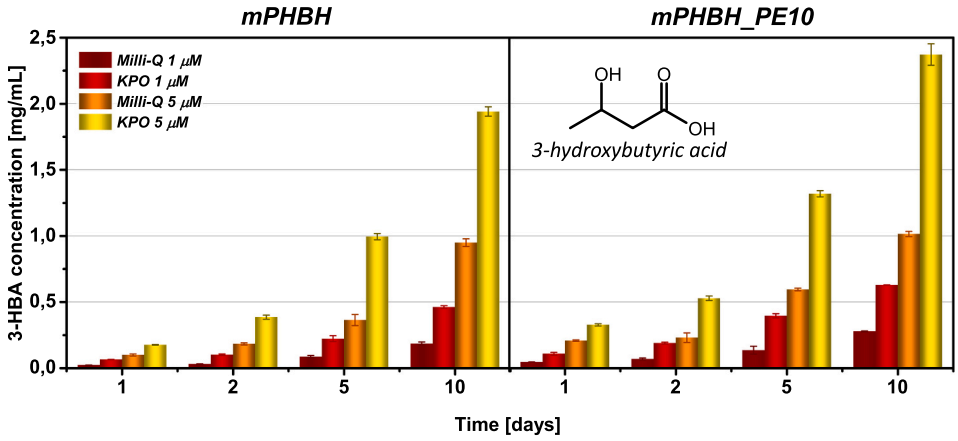

Fig. 9. 3-HBA concentration in the supernatant recovered from enzymatic hydrolysis of mPHBH and mPHBH_PE10 porous films in KPO 0.1 M pH = 8.0.

efficient absorbers of a cationic dye, whose retention capacity reached the highest value in the films containing the additive produced from the greatest PE amount and thus characterized by the highest content of hydroxyl functionalities.

Moreover, the same formulation proved to be capable of retaining also a metal cation, namely Pd^{2+}, which is generally used in homogeneous catalysis. The activity of the system consisting of Pd clusters formed as a result of the reduction of the metal precursor on the porous substrate was detected in the hydrogenation reaction of a model compound, trans-stilbene, and showed activity comparable to that of a conventional supported catalyst, demonstrating the possibility of using the developed films both as a homogeneous catalyst absorber and as a heterogeneous catalyst support.

Finally, the oligomer-containing films exhibited better enzymatic degradability than those prepared using neat PHBH, with tunable degradation rates by varying the additive type or enzyme medium. Overall, the main advantage of this upcycling approach relies on the direct applicability of the produced branched PHBH oligomers without further purification steps, which is a significant improvement over the standard chemical recycling approaches where energy- and solvent-intensive processes could hinder their sustainability and scalability. These properties combined with the simple and scalable production process pave the way for an innovative recycling strategy, not only for PHBH, but also for other PHA and polyesters, making the developed approach interesting from both a scientific and an industrial point of view. Based on the encouraging results of the films containing the developed additives, further studies on biodegradation, cytotoxicity, and scaling of the process will be conducted in the future.

CRediT authorship contribution statement

Giacomo Damonte: Validation, Data curation, Writing – original draft, Methodology, Investigation. **Martina Cozzani:** Data curation, Investigation. **Marco Ozenda:** Investigation. **Chiara Siracusa:** Investigation. **Maria Jose Calandri:** Investigation. **Alessandro Pellis:** Methodology, Funding acquisition, Writing – review & editing. **Georg M. Guebitz:** Writing – review & editing, Methodology. **Orietta Monticelli:** Funding acquisition, Writing – review & editing, Supervision, Conceptualization.

Declaration of competing interest

There are no conflicts to declare.

Acknowledgements

Funded by PLA-VIT project (P20229KM4Z) (European Union Next-Generation EU through the PRIN (Progetti di Ricerca di Rilevante Interesse Nazionale) PNRR (Piano Nazionale di Ripresa e Resilienza) 2022 call from the Italian Ministry of Education and Research (MUR)) and ERC CIRCULARIZE (101114664) (European Union). Views and opinions expressed are, however, those of the author(s) only and do not necessarily reflect those of the European Union or the European Research Council. Neither the European Union nor the granting authority can be held responsible for them.

Appendix A. Supplementary data

Supplementary data to this article can be found online at https://doi.org/10.1016/j.ijbiomac.2025.145457.

Data availability

The authors confirm that the data supporting the findings of this study are available within the article and its ESI.

References

[1] F. Muneer, I. Rasul, F. Azeem, M.H. Siddique, M. Zubair, H. Nadeem, Microbial Polyhydroxyalkanoates (PHAs): efficient replacement of synthetic polymers, J. Polym. Environ. 28 (2020) 2301–2323, https://doi.org/10.1007/s10924-020-01772-1.
[2] K.W. Meereboer, M. Misra, A.K. Mohanty, Review of recent advances in the biodegradability of polyhydroxyalkanoate (PHA) bioplastics and their composites, Green Chem. 22 (2020) 5519–5558, https://doi.org/10.1039/d0gc01647k.
[3] K. Eraslan, C. Aversa, M. Nofar, M. Barletta, A. Gisario, R. Salehiyan, Y.A. Goksu, Poly(3-hydroxybutyrate-co-3-hydroxyhexanoate) (PHBH): synthesis, properties, and applications - a review, Eur. Polym. J. 167 (2022) 111044, https://doi.org/10.1016/j.eurpolymj.2022.111044.
[4] M. Koller, Biodegradable and biocompatible polyhydroxy-alkanoates (PHA): auspicious microbial macromolecules for pharmaceutical and therapeutic applications, Molecules 23 (2018) 362, https://doi.org/10.3390/molecules23020362.
[5] J. Yu, L.X.L. Chen, The greenhouse gas emissions and fossil energy requirement of bioplastics from cradle to gate of a biomass refinery, Environ. Sci. Technol. 42 (2008) 6961–6966, https://doi.org/10.1021/es7032235.
[6] F.M. Lamberti, L.A. Román-Ramírez, J. Wood, Recycling of bioplastics: routes and benefits, J. Polym. Environ. 28 (2020) 2551–2571, https://doi.org/10.1007/s10924-020-01795-8.
[7] A.Z. Naser, I. Deiab, B.M. Darras, Poly(lactic acid) (PLA) and polyhydroxyalkanoates (PHAs), green alternatives to petroleum-based plastics: a review, RSC Adv. 11 (2021) 17151–17196, https://doi.org/10.1039/D1RA02390J.
[8] C.D. Usurelu, S. Badila, A.N. Frone, D.M. Panaitescu, Poly(3-hydroxybutyrate) nanocomposites with cellulose nanocrystals, Polymers 14 (2022) 1974, https://doi.org/10.3390/polym14101974.
[9] P. Feijoo, K. Samaniego-Aguilar, E. Sánchez-Safont, S. Torres-Giner, J.M. Lagaron, J. Gamez-Perez, L. Cabedo, Development and characterization of fully renewable and biodegradable polyhydroxyalkanoate blends with improved thermoformability, Polymers 14 (2022) 2527, https://doi.org/10.3390/polym14132527.
[10] M. Plouzeau, I. Belyamani, K. Fatyeyeva, S. Marais, Y. Kobzar, L. Cauret, Recyclability of poly(hydroxybutyrate-co-hydroxyhexanoate) (PHBH) for food

packaging applications, Food Packag. Shelf Life 40 (2023) 101170, https://doi.org/10.1016/j.fpsl.2023.101170.
[11] W. Adachi, S. Kumagai, Z. Shao, Y. Saito, T. Yoshioka, Selective recovery of pyrolyzates of biodegradable (PLA, PHBH) and common plastics (HDPE, PP, PS) during co-pyrolysis under slow heating, Sci. Rep. 14 (2024) 16476, https://doi.org/10.1038/s41598-024-67330-0.
[12] Z. Shao, S. Kumagai, Y. Saito, T. Yoshioka, Characteristics of the steam degradation of poly(lactic acid) and poly(3-hydroxybutyrate-co-3-hydroxyhexanoate), Polym. J. 56 (2024) 455–462, https://doi.org/10.1038/s41428-024-00883-z.
[13] G. Damonte, A. Vallin, L. Giribaldi, A. Pellis, M. Hakkarainen, S. Subramaniyan, P. Campaner, O. Monticelli, A sustainable approach to recycling of polylactic acid with environmentally friendly reagents, Sustain. Mater. Technol. 43 (2025) e01320, https://doi.org/10.1016/j.susmat.2025.e01320.
[14] E. Cheung, C. Alberti, S. Bycinskij, S. Enthaler, Zinc-catalyzed chemical recycling of poly(ϵ-caprolactone) applying transesterification reactions, ChemistrySelect 6 (2021) 8063–8067, https://doi.org/10.1002/slct.202004294.
[15] Y. Dong, F. Lin, T. Zhao, M. Wang, D. Ning, X. Hao, Y. Zhang, D. Zhou, Y. Zhao, X. Chen, B. Wang, Dispersion and lubrication of zinc stearate in polypropylene/sodium 4-[(4-chlorobenzoyl) amino] benzoate nucleating agent composite, Polymers 16 (2024) 1942, https://doi.org/10.3390/polym16131942.
[16] M. Melchiorre, M.E. Cucciolito, M. Di Serio, F. Ruffo, O. Tarallo, M. Trifuoggi, R. Esposito, Homogeneous catalysis and heterogeneous recycling: a simple Zn(II) catalyst for green fatty acid esterification, ACS Sustain. Chem. Eng. 9 (2021) 6001–6011, https://doi.org/10.1021/acssuschemeng.1c01140.
[17] C. Liu, W. Qiao, C. Wang, H. Wang, Y. Zhou, S. Gu, W. Xu, Y. Zhuang, J. Shi, H. Yang, Effect of poly (lactic acid) porous membrane prepared via phase inversion induced by water droplets on 3T3 cell behavior, Int. J. Biol. Macromol. 183 (2021) 2205–2214, https://doi.org/10.1016/j.ijbiomac.2021.05.197.
[18] M.M.H. Mizan, M. Rastgar, H. Sultana, P. Karami, M. Sadrzadeh, Green polycaprolactone/sulfonated Kraft lignin phase inversion membrane for dye/salt separation, J. Memb. Sci. 702 (2024) 122806, https://doi.org/10.1016/j.memsci.2024.122806.
[19] T.A. Otitoju, C.-H. Kim, M. Ryu, J. Park, T.-K. Kim, Y. Yoo, H. Park, J.-H. Lee, Y. H. Cho, Exploring green solvents for the sustainable fabrication of bio-based polylactic acid membranes using nonsolvent-induced phase separation, J. Clean. Prod. 467 (2024) 142905, https://doi.org/10.1016/j.jclepro.2024.142905.
[20] R.A. Milescu, A. Zhenova, M. Vastano, R. Gammons, S. Lin, C.H. Lau, J.H. Clark, C. R. McElroy, A. Pellis, Polymer chemistry applications of cyrene and its derivative cygnet 0.0 as safer replacements for polar aprotic solvents, ChemSusChem 14 (2021) 3367–3381, https://doi.org/10.1002/cssc.202101125.
[21] T. Marino, F. Galiano, A. Molino, A. Figoli, New frontiers in sustainable membrane preparation: cyrene™ as green bioderived solvent, J. Memb. Sci. 580 (2019) 224–234, https://doi.org/10.1016/j.memsci.2019.03.034.
[22] S. Shetty, N. Baig, R. Bargakshatriya, S.K. Pramanik, B. Alameddine, High uptake of the carcinogenic pararosaniline hydrochloride dye from water using carbazole-containing conjugated copolymers synthesized from a one-pot cyclopentannulation reaction, ACS Appl. Mater. Interfaces 15 (2023) 28149–28157, https://doi.org/10.1021/acsami.3c05639.
[23] J. Kowalska, A. Jeżewska, Determination of pararosaniline hydrochloride in workplace air, Environ. Monit. Assess. 191 (2019) 444, https://doi.org/10.1007/s10661-019-7568-z.
[24] S.W. Acker L., K.-G. Bergner, W. Diemair, W. Heimann, F. Kiermeier, J. Schormüller, Souci, Handbuch der Lebensmittelchemie, herausgeg. von L. Acker, K.-G. Bergner, W. Diemair, W. Heimann, F. Kiermeier, J. Schormüller und S. W. Souci, Gesamtredaktion J. Schormüller, Bd. II/2. Teil: Analytik der Lebensmittel. Nachweis und Bestimmung von Lebensmit, Food/Nahrung 11 (1967) 532, https://doi.org/10.1002/food.19670110612.
[25] J. Mai, C.M. Chan, J. Colwell, S. Pratt, B. Laycock, Characterisation of end groups of hydroxy-functionalised scl-PHAs prepared by transesterification using ethylene glycol, Polym. Degrad. Stab. 205 (2022) 110123, https://doi.org/10.1016/j.polymdegradstab. 2022.110123.
[26] F. Dai, Q. Zhuang, G. Huang, H. Deng, X. Zhang, Infrared spectrum characteristics and quantification of OH groups in coal, ACS Omega 8 (2023) 17064–17076, https://doi.org/10.1021/acsomega.3c01336.
[27] L. Tripathi, L.-P. Wu, J. Chen, G.-Q. Chen, Synthesis of diblock copolymer poly-3-hydroxybutyrate-block-poly-3-hydroxyhexanoate [PHB-b-PHHx] by a β-oxidation weakened Pseudomonas putida KT2442, Microb. Cell Fact. 11 (2012) 44, https://doi.org/10.1186/1475-2859-11-44.
[28] K.W. Scott, Criteria for random degradation of linear polymers, J. Polym. Sci. Polym. Symp. 46 (1974) 321–334, https://doi.org/10.1002/polc.5070460124.
[29] M.I.A. Majid, J. Ismail, L.L. Few, C.F. Tan, The degradation kinetics of poly(3-hydroxybutyrate) under non-aqueous and aqueous conditions, Eur. Polym. J. 38 (2002) 837–839, https://doi.org/10.1016/S0014-3057(01)00226-9.
[30] Z. Špitalský, I. Lacík, E. Lathová, I. Janigová, I. Chodák, Controlled degradation of polyhydroxybutyrate via alcoholysis with ethylene glycol or glycerol, Polym. Degrad. Stab. 91 (2006) 856–861, https://doi.org/10.1016/j.polymdegradstab.2005.06.019.
[31] J. Ivorra-Martinez, I. Verdu, O. Fenollar, L. Sanchez-Nacher, R. Balart, L. Quiles-Carrillo, Manufacturing and properties of binary blend from bacterial polyester poly(3-hydroxybutyrate-co-3-hydroxyhexanoate) and poly(caprolactone) with improved toughness, Polymers 12 (2020) 1118, https://doi.org/10.3390/polym12051118.
[32] Y. Farrag, L. Barral, O. Gualillo, D. Moncada, B. Montero, M. Rico, R. Bouza, Effect of different plasticizers on thermal, crystalline, and permeability properties of poly (3–hydroxybutyrate–co−3–hydroxyhexanoate) films, Polymers 14 (2022) 3503, https://doi.org/10.3390/polym14173503.
[33] Y. Qiu, X. Ma, Crystallization, mechanical and UV protection properties of graphene oxide/poly(3-hydroxybutyrate-co-3-hydroxyhexanoate) biocomposites, J. Mater. Sci. 54 (2019) 14388–14399, https://doi.org/10.1007/s10853-019-03951-5.
[34] M. Melchiors, H. Keul, H. Höcker, Depolymerization of poly[(R)-3-hydroxybutyrate] to cyclic oligomers and polymerization of the cyclic trimer: an example of thermodynamic recycling, Macromolecules 29 (1996) 6442–6451, https://doi.org/10.1021/ma9604350.
[35] A. Dehban, F. Hosseini Saeedavi, A. Kargari, A study on the mechanism of pore formation through VIPS-NIPS technique for membrane fabrication, J. Ind. Eng. Chem. 108 (2022) 54–71, https://doi.org/10.1016/j.jiec.2021.12.023.
[36] I.V. Maggay, M.-L. Yu, D.-M. Wang, C.-H. Chiang, Y. Chang, A. Venault, Strategy to prepare skin-free and macrovoid-free polysulfone membranes via the NIPS process, J. Memb. Sci. 655 (2022) 120597, https://doi.org/10.1016/j.memsci.2022.120597.
[37] H.H. Wang, J.T. Jung, J.F. Kim, S. Kim, E. Drioli, Y.M. Lee, A novel green solvent alternative for polymeric membrane preparation via nonsolvent-induced phase separation (NIPS), J. Memb. Sci. 574 (2019) 44–54, https://doi.org/10.1016/j.memsci.2018.12.051.
[38] M. Cozzani, P.F. Ferrari, G. Damonte, A. Pellis, O. Monticelli, On the development of polylactic acid/polycaprolactone blended films with high retention capacity, Macromol. Biosci. (2024) 1–12, https://doi.org/10.1002/mabi.202400272.
[39] X. Tan, D. Rodrigue, A review on porous polymeric membrane preparation. Part I: production techniques with polysulfone and poly(vinylidene fluoride), Polymers 11 (2019) 1160, https://doi.org/10.3390/polym11071160.
[40] C.A. Smolders, A.J. Reuvers, R.M. Boom, I.M. Wienk, Microstructures in phase-inversion membranes. Part 1. Formation of macrovoids, J. Memb. Sci. 73 (1992) 259–275, https://doi.org/10.1016/0376-7388(92)80134-6.
[41] I. Noda, P.R. Green, M.M. Satkowski, L.A. Schechtman, Preparation and properties of a novel class of polyhydroxyalkanoate copolymers, Biomacromolecules 6 (2005) 580–586, https://doi.org/10.1021/bm049472m.
[42] A. Pawlak, J. Krajenta, Entanglements of macromolecules and their influence on rheological and mechanical properties of polymers, Molecules 29 (2024) 3410, https://doi.org/10.3390/molecules29143410.
[43] G. Damonte, B. Barsanti, A. Pellis, G.M. Guebitz, O. Monticelli, On the effective application of star-shaped polycaprolactones with different end functionalities to improve the properties of polylactic acid blend films, Eur. Polym. J. 176 (2022) 111402, https://doi.org/10.1016/j.eurpolymj.2022.111402.
[44] T.L. do A. Montanheiro, L.S. Montagna, V. Patrulea, O. Jordan, G. Borchard, R. G. Ribas, T.M.B. Campos, G.P. Thim, A.P. Lemes, Enhanced water uptake of PHBV scaffolds with functionalized cellulose nanocrystals, Polym. Test. 79 (2019) 106079, https://doi.org/10.1016/j.polymertesting.2019.106079.
[45] C.Y. Tang, D.Z. Chen, T.M. Yue, K.C. Chan, C.P. Tsui, P.H.F. Yu, Water absorption and solubility of PHBHV/HA nanocomposites, Compos. Sci. Technol. 68 (2008) 1927–1934, https://doi.org/10.1016/j.compscitech.2007.12.003.
[46] N.F. Ansari, A.A. Amirul, Preparation and characterization of polyhydroxyalkanoates macroporous scaffold through enzyme-mediated modifications, Appl. Biochem. Biotechnol. 170 (2013) 690–709, https://doi.org/10.1007/s12010-013-0216-0.
[47] J. Chen, Z. Zhang, B. Li, F. Li, Y. Wang, M. Zhao, I.D. Gridnev, T. Imamoto, W. Zhang, Pd(OAc)2-catalyzed asymmetric hydrogenation of sterically hindered N-tosylimines, Nat. Commun. 9 (2018) 5000, https://doi.org/10.1038/s41467-018-07462-w.
[48] A. Blangiardo, G. Lagomarsino, A. Basso, P. Canepa, O. Cavalleri, S. Rossi, O. Monticelli, Preparation, application and recycling of a catalytic microflow reactor based on polylactic acid, Appl. Surf. Sci. 569 (2021) 151019, https://doi.org/10.1016/j.apsusc.2021.151019.
[49] O. Monticelli, S. Russo, R. Campagna, B. Voit, Preparation and characterisation of blends based on polyamide 6 and hyperbranched aramids as palladium nanoparticle supports, Polymer 46 (2005) 3597–3606, https://doi.org/10.1016/j.polymer.2005.03.029.
[50] L. Gardella, A. Basso, M. Prato, O. Monticelli, PLA/POSS nanofibers: a novel system for the immobilization of metal nanoparticles, ACS Appl. Mater. Interfaces 5 (2013) 7688–7692, https://doi.org/10.1021/am402280j.
[51] V. Ferrario, A. Pellis, M. Cespugli, G. Guebitz, L. Gardossi, Nature inspired solutions for polymers: will cutinase enzymes make polyesters and polyamides greener? Catalysts 6 (2016) 205, https://doi.org/10.3390/catal6120205.
[52] Q. Huang, S. Kimura, T. Iwata, Thermal embedding of humicola insolens cutinase: a strategy for improving polyester biodegradation in seawater, Biomacromolecules 24 (2023) 5836–5846, https://doi.org/10.1021/acs.biomac.3c00835.